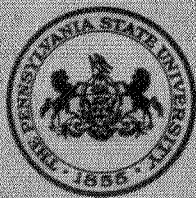THE PENNSYLVANIA
STATE UNIVERSITY
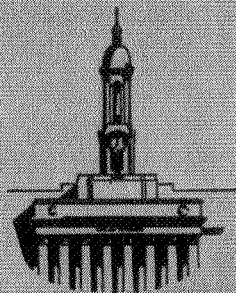
IONOSPHERIC RESEARCH

Scientific Report No. 365

THE COMPETITIVE REACTION OF O(¹D) WITH OZONE AND NITROUS OXIDE

by

C. S. Goldman

November 1, 1970

IONOSPHERE RESEARCH LABORATORY

University Park, Pennsylvania   NASA Grant NGL-009-003

Ionospheric Research

NASA Grant NGL-009-003

Scientific Report

on

"The Competitive Reaction of O(^{1}D) with
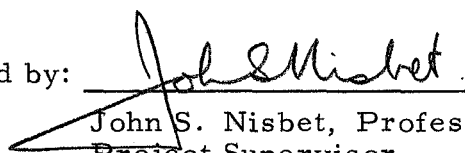Ozone and Nitrous Oxide"
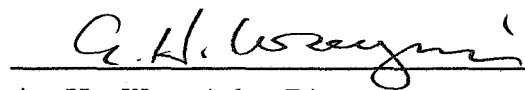
by

C. S. Goldman

November 1, 1970

Scientific Report No. 365

Ionosphere Research Laboratory

Submitted by: _____

John S. Nisbet, Professor of Electrical Engineering
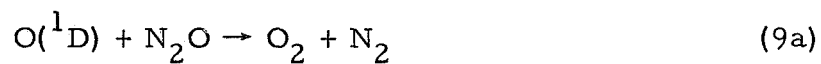Project Supervisor

Approved by: _____

A. H. Waynick, Director
Ionosphere Research Laboratory

The Pennsylvania State University

College of Engineering

Department of Electrical Engineering

ABSTRACT

The competitive reactions of $O(^1D)$ atoms with ozone and nitrous oxide were studied

$$O(^1D) + O_3 \rightarrow 2O_2 \tag{2}$$

$$O(^1D) + N_2O \rightarrow O_2 + N_2 \tag{9a}$$

$$O(^1D) + N_2O \rightarrow 2NO \tag{9b}$$

The values of k_2/k_9 and k_{9a}/k_{9b} were determined from the photolysis of ozone at 2288 and 2537 A. Experiments show that the value of k_{9a}/k_{9b} depends on the pressure of added helium. This result is interpreted in terms of the excess translational energy possessed by the $O(^1D)$ atoms.

TABLE OF CONTENTS

CHAPTER 1

INTRODUCTION

The $O(^1D)$ Atom

One of the most important constituents of the upper atmosphere is the $O(^1D)$ atom. The oxygen red lines, due to the radiative transition of this electronically excited atom to its $O(^3P)$ ground state are a prominant feature of the airglow.

Below 70 km. the principle source of $O(^1D)$ in the atmosphere is the photodissociation of ozone by ultra-violet radiation from sunlight. DeMore and Raper[1] have shown that at wavelengths less than 3000 A for every ozone photolyzed, an $O(^1D)$ atom is formed. In the atmosphere, for an overhead sun, the concentration of $O(^1D)$ due to the photolysis of ozone reaches a maximum at an altitude of 50 km.[2] Above 90 km. the concentration of $O(^1D)$ begins to increase, due to the photolysis of oxygen molecules by light of wavelengths less than 1750 A. At the altitude of 120 km. the concentration of atomic oxygen becomes greater than that of molecular oxygen.[3]

The principal loss processes for the $O(^1D)$ atom are the deactivation by oxygen and nitrogen. The radiative transition to the ground state is spin forbidden, the radiative lifetime of the $O(^1D)$ atom is of the order of 100 seconds. Therefore, it is not important in comparison to the rates of deactivation and reaction, in accounting for the loss of $O(^1D)$ in the upper atmosphere. Table 1 shows the photo-equilibrium concentration of $O(^1D)$ for an overhead sun as a function of altitude.

TABLE 1

## CONCENTRATION OF $O(^1D)$ FOR AN OVERHEAD SUN-EQUILIBRIUM CONDITIONS[3]

Altitude (km.)	Atoms/cm^3	Altitude (km.)	Atoms/cm^3
20	2.5	65	2.0×10^2
25	1.1×10^1	70	1.2×10^2
30	4.4×10^1	95	4.0×10^2
35	1.5×10^2	100	1.0×10^3
40	4.4×10^2	105	2.0×10^3
45	7.8×10^2	110	4.0×10^3
50	7.9×10^2	115	5.0×10^3
55	5.6×10^2	120	4.0×10^3
60	3.3×10^2		

Other species, present in the upper atmosphere in trace amounts that could be photolyzed to give $O(^1D)$ atoms, are N_2O, NO, NO_2, and CO_2. While all the above compounds, with the exception of NO, have been used to produce $O(^1D)$ atoms in the laboratory;[4-7] their contribution to the concentration of $O(^1D)$ atoms in the atmosphere is minor. More detailed information on the production and reactions of $O(^1D)$ atoms can be found in an excellent review article by McGrath and McGarvey.[8]

The Photolysis of Ozone

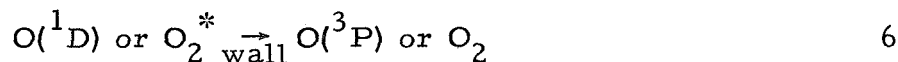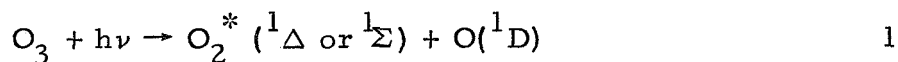A common source of oxygen atoms in the laboratory as well as in the atmosphere, is the photolysis of ozone. It has been shown[9] that the photolysis of ozone with red light ($\lambda > 6000$ A) results in the formation of the $O(^3P)$ ground state oxygen atom and a molecule of ground state oxygen. With radiation below 3000 A the photolysis of ozone results in the production of the $O(^1D)$ atom and an excited

oxygen molecule:

$$O_3(^1A) + h\nu \rightarrow O(^1D) + O_2^* \quad (\lambda < 3100) \qquad 1$$
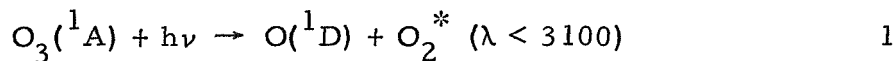
There is still considerable controversy over the electronic

state of the excited oxygen molecule formed in the photolysis of

ozone, although some recent evidence points to the formation of the

$O_2(^1\Delta)$ state even at 3130 A.[10] The values in Table 2, calculated using

the thermodynamical values given in Table 3 and Table 4, indicate the

wavelength necessary to produce the various species found in the

photolysis of ozone.

It has been shown[13] that below 3000 A, the quantum yield for

the formation of $O(^1D)$ is unity and that the quantum yield for the

disappearance of ozone is greater than one. This indicates that the

mechanism for the photolysis of ozone involves a chain. The

mechanism proposed by Norrish and Wayne[14] for the ultra-violet

photolysis of ozone is:

$$O_3 + h\nu \rightarrow O_2^* \; (^1\Delta \text{ or } ^1\Sigma) + O(^1D) \qquad 1$$

$$O(^1D) + O_3 \rightarrow O_2^\dagger + O_2 \qquad 2$$

$$O_2^\dagger + O_3 \rightarrow 2O_2 + O(^1D) \qquad 3$$

$$O_2^* + O_3 \rightarrow 2O_2 + O(^3P) \qquad 4$$

$$O(^3P) + O_3 \rightarrow 2O_2 \qquad 5$$

$$O(^1D) \text{ or } O_2^* \xrightarrow[\text{wall}]{} O(^3P) \text{ or } O_2 \qquad 6$$

where $O_2^\dagger$ is an energy rich molecule of oxygen (not $^1\Delta$ or $^1\Sigma$).

TABLE 2

WAVELENGTH (A) BELOW WHICH IT IS ENERGETICALLY
POSSIBLE TO PRODUCE THE INDICATED SPECIES
FROM O_3 PHOTOLYSIS

Species	$O_2(^3\Sigma_g^-)$	$O_2(^1\Delta_g)$	$O_2(^1\Sigma_g^+)$
$O(^3P)$	11,000	6110[a]	4600[a]
$O(^1D)$	4,000[a]	3100	2660
$O(^1S)$	2,330[a]	1995	1800

a. Spin forbidden transition

TABLE 3

THERMODYNAMIC VALUES OF INTEREST
BOND DISSOCIATION ENERGIES[11]

Bond	$\Delta H^o_{298.2}$, Kcal/mole
O_2-O	26
N_2-O	40
N-NO	115
O-O	119
O-NO	73
OC-O	127

TABLE 4

ELECTRONIC LEVELS OF INTEREST[12]

Energy Level	Kcal/mole
$O(^3P)$	0.0
$O(^1D)$	45.4
$O(^1S)$	96.6
$O_2(^3\Sigma)$	0.0
$O_2(^1\Delta)$	20.8
$O_2(^1\Sigma)$	36.2

The Photolysis of Nitrous Oxide

The photolysis of nitrous oxide has been studied by Noyes and co-workers[15-17] who found two different dissociation mechanisms:

$$N_2O + h\nu \rightarrow N_2 + O \qquad 7$$

$$N_2O + h\nu \rightarrow NO + N. \qquad 8$$

With radiation of either 1849 A or 2139 A, reaction 7 is the predominate one and the oxygen atom formed is $O(^1D)$.[18-22]

The oxygen atom formed will then further react with the nitrous oxide:

$$O(^1D) + N_2O \rightarrow N_2 + O_2 \qquad 9a$$

$$O(^1D) + N_2O \rightarrow 2NO. \qquad 9b$$

The ratio k_{9a}/k_{9b} has been estimated by various investigators to be anywhere from 0.5 to 1.44. The estimates for this ratio are contained in a recent paper from this research group.[23]

The Present Investigation

The present investigation's purpose was several fold. It was hoped to determine the ratio of k_{9a}/k_{9b} and to study the competitive rate of reaction of $O(^1D)$ with ozone and nitrous oxide $(k_2/k_9; \; k_9 = k_{9a} + k_{9b})$. In this work the source of the $O(^1D)$ was from the photolysis of ozone at 2288 A and 2537 A. Due to the low absorbance of nitrous oxide at these wavelengths almost all of the $O(^1D)$ formed in the photolysis of mixtures of ozone and nitrous oxide came from the ozone.

Another goal of the present work was to observe the effect of added gases, that quench only excess translational energy, on the ratios k_2/k_9 and k_{9a}/k_{9b}. This effect had not been reported previously, and it was hoped that it might help clarify some of the seemingly inconsistent results obtained in the previous studies involving $O(^1D)$.

CHAPTER II

EXPERIMENTAL

The High-Vacuum System

The high-vacuum system was constructed of Pyrex tubing in the normal fashion. The location of the various components are shown in Figure 1. Since ozone reacts with both mercury and grease, the vacuum system was kept mercury and grease free. All the stopcocks on the main manifolds were West Glass Teflon stopcocks. The pumping system consisted of a three-stage oil diffusion pump and a Welch Duoseal oil pump. Pressures were measured on a NRC Alphatron Gauge which was calibrated for the different reactants with a sulfuric acid manometer.

The Optical System

The reaction vessel used was a cylindrical quartz cell, 100 mm. in length and 50 mm. in diameter. The cell was clamped into place in such a way that the radiation from the lamp used to monitor the ozone concentration traversed the length of the cell, and the lamp used for the photolysis of the reactants was at right angle to the long axis of the reaction vessel. This is illustrated in Figure 2.

The radiation sources used were a Phillips low-pressure mercury lamp, model 93109E, and a 25 watt Phillips cadmium lamp model 93107E. The lamp used for monitoring the ozone concentration was a 150 watt Osram xenon arc lamp.

A monochromatic wavelength, used for monitoring the ozone, was obtained by isolating a line of the xenon lamp continuim with a

TO OIL
DIFFUSION PUMP

TO ALPHATRON
GAUGE

2 LITER
STORAGE
BULB

TO VACUUM
PUMP

U TRAP

TESLA COIL

U TRAP

TO GAS
CHROMATOGRAPH
SYSTEM

COIL
TRAP

SULFURIC ACID
MANOMETER

1 LITER
OZONE STORAGE
BULB

⊗ - TEFLON STOPCOCKS

BLANK
REACTION
CELL

REACTION
CELL

FIGURE 1

VACUUM LINE

PHILLIPS LAMP
(CADMIUM OR MERCURY)

CORNING 9-30 FILTER

CHLORINE FILTER

CORNING CS 7-54
FILTER

XENON
LAMP

QUARTZ
LENSES

JARRELL-ASH
MONOCHROMATOR

REACTION
CELL

QUARTZ
LENSE

RCA 935
PHOTOTUBE
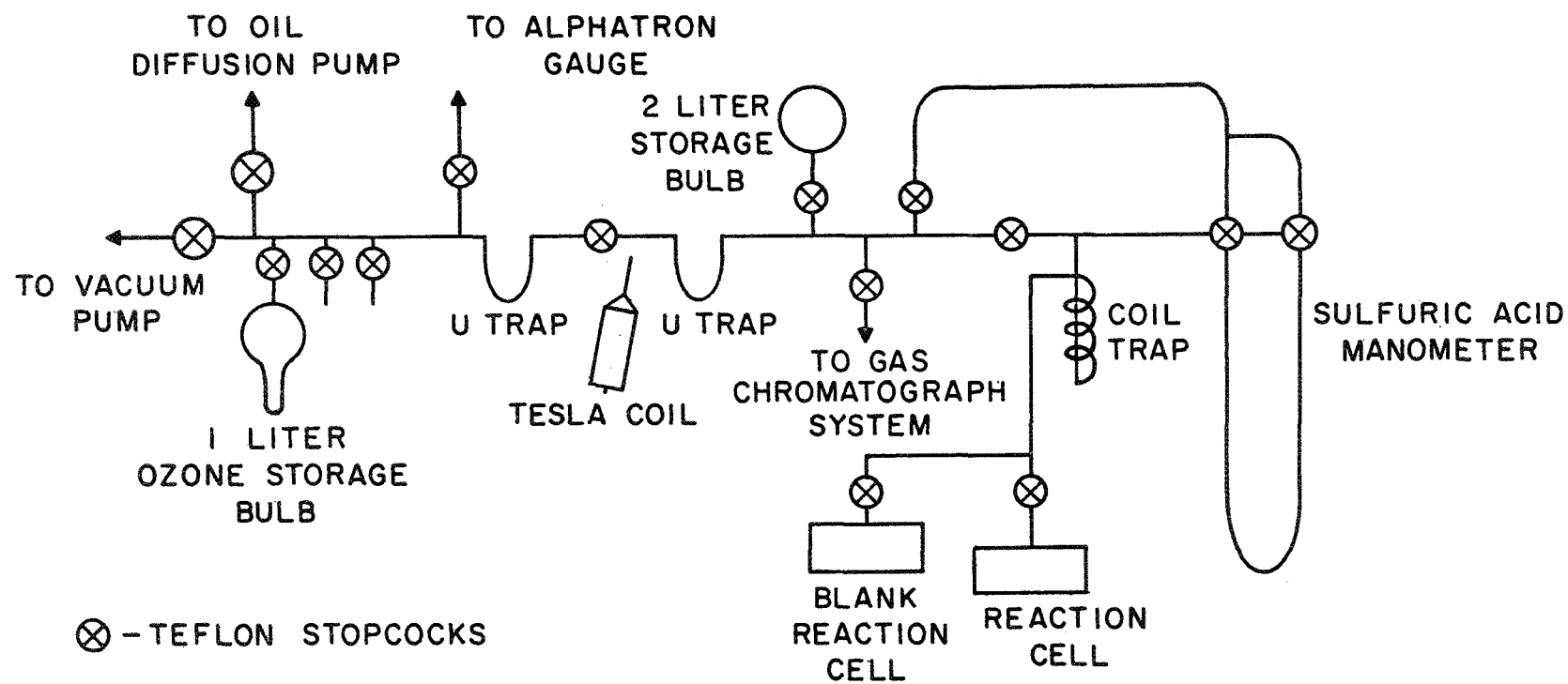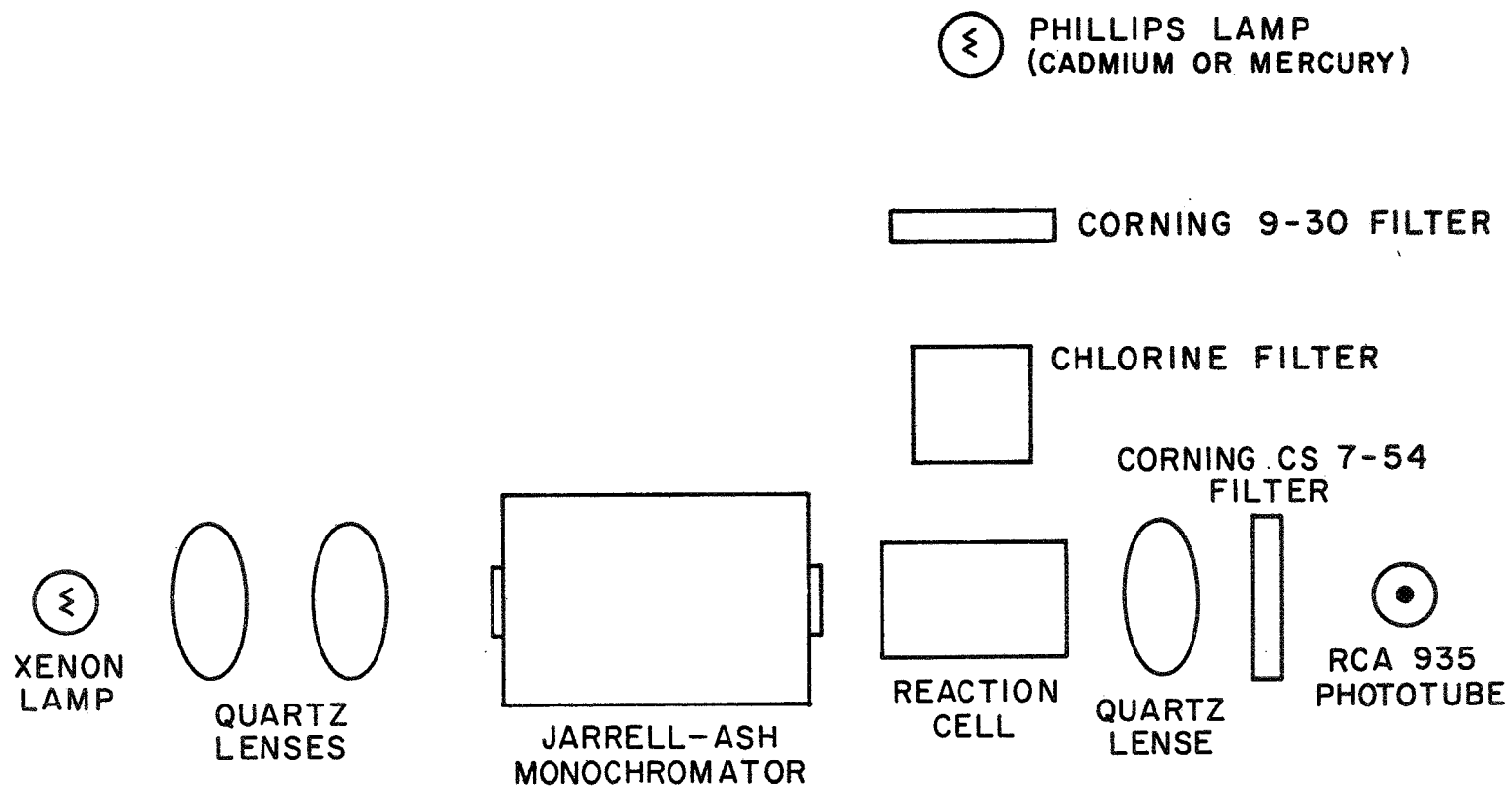
FIGURE 2

OPTICAL SYSTEM

Jarrell-Ash, 1/4 meter, Ebert monochromator, model 82-410, and a Corning CS 7-54 filter. This wavelength was monitored by the use of a R.C.A. 935 phototube. The photolyzing wavelengths were isolated by passing the radiation through a Corning 9-30 filter to remove radiation below 2200 A and a five cm. quartz cell containing 300 torr of chlorine to remove radiation between 2700 and 4000 A.

The effective emission of the filtered mercury lamp was a line at 2537 A. For the filtered cadmium lamp there was a strong line at 2288 A and another line less than five percent as strong at 2265 A. The absorbed intensity was approximately the same for both lamps. The high intensity points at 2288 A were done by removing the Corning 9-30 filter.

The output of the lamps was measured at both wavelengths by using a mixture of CF_3I and O_2 as a chemical actinometer.[24] CF_2O is produced which quantitatively converts to CO_2 in the gas chromatograph; $\Phi\{CO_2\} = 1.0$ at 3130 A. This actinometry system was compared to the results obtained by using HBr and HI as chemical actinometers at 2288 A and 2537 A respectively; for both cases $\Phi\{H_2\} = 1.0$.[11] The results indicated that the CF_3I and O_2 mixture could be used for chemical actinometry at the wavelengths used in this work. The advantage in using this system for actinometry rather than the hydrogran halides is that small amounts of the hydrogen halides were absorbed by the O-rings of the Teflon stopcocks and resulted in irreproducible results when O_3 was photolyzed. Using CF_3I as an actinometer, it was determined that the output of both lamps were reproducible to better than five percent.

Materials and Purifications

Ozone was made by passing an electric discharge through oxygen (Air Products Research Grade). The ozone produced was collected over liquid nitrogen, the excess oxygen pumped away, and then the ozone was degassed and distilled in vacuo at $-186^{\circ}C$ (liquid argon). Before each run the ozone was degassed over liquid nitrogen. In this way the ozone produced was over 95 percent pure, with the only observable impurity being oxygen.

Nitrous oxide (Matheson) was degassed over liquid nitrogen. Gas chromatography indicated that the nitrous oxide purified in this manner contained no nitrogen or any interfering foreign matter.

Helium was purified the same way as the helium used in the gas chromatography system.

Trifluromethyl-iodide (Peninsular) was passed through an Ascarite trap and degassed at liquid nitrogen temperature. Analysis by gas chromatography showed carbon dioxide less than 10 ppm.

The Gas Chromatograph

Gas chromatography was used for the quantitative analysis of products. Two separate gas chromatography systems were used, one for the condensible products (at $-196^{\circ}C$) and one for the non-condensible products (at $-196^{\circ}C$). The only condensible product analyzed was the CO_2 which was formed in the actinometry runs. In analyzing for CO_2 the condensibles were collected in a demountable U-trap, the non-condensibles pumped away, and then the CO_2 was analyzed on a separate gas chromatograph system not connected to the high-vacuum line.

The non-condensibles which were formed in the photolysis of the ozone- nitrous oxide mixtures were oxygen and nitrogen; they were analyzed on a gas chromatograph system that was connected to the high-vacuum line by a four way glass stopcock. The sampler of this system consisted of a 10 foot coil of 12 mm. glass tubing. The set up and operation of this gas chromatograph are illustrated in Figure 3.

It was found that the calibration of the gas chromatograph system were affected by the addition of helium to the reaction cell. When calibrations were done for pressures of nitrogen greater than 50 microns, the results were 10 to 25 percent greater in the presence of helium. However, in the range of pressures measured after each run, 20 microns or less, it was found that the addition of helium to the reaction mixtures made no appreciable difference on the calibrations. Therefore, the same calibrations were used for nitrogen in the presence of helium as when there was no helium present.

Both of the gas chromatographs used consisted of a detector (Gow Mac Model 10-777), a power supply (Gow Mac Model 40-012), and a recorder (Texas Instrument Servo-Riter II). The detector was run at 0° C, and a constant current of 15 milliamperes was maintained by the power supply. Helium, passed through a column of Ascarite and indicating drierite, was used as the carrier gas.

The columns used were a 10 foot 1/4 inch ID copper tube containing 5A molecular sieves for the analysis of the non-condensibles and a 12 foot 1/4 inch ID copper column containing Porapak Q for the analysis of CO_2.
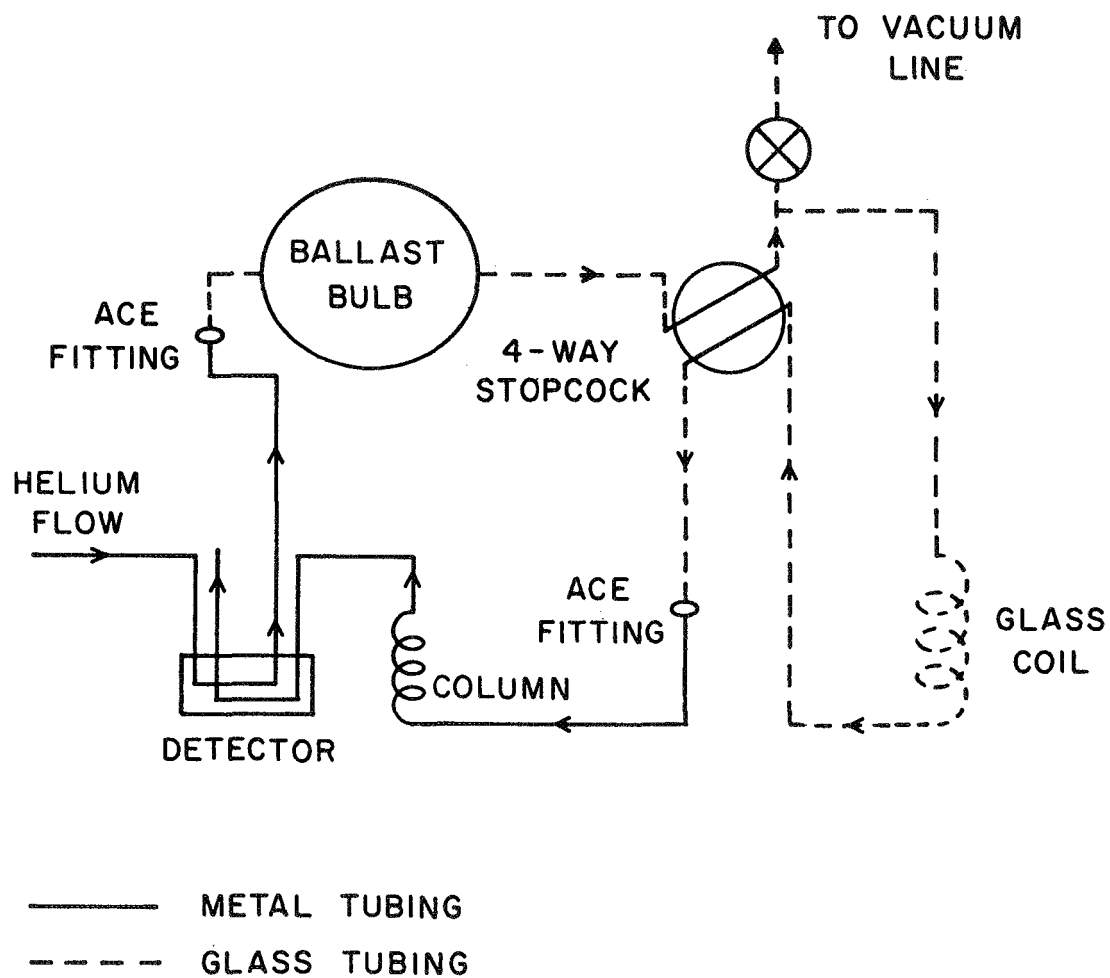
FIGURE 3

GAS CHROMATOGRAPH

Operational Procedures

A measured pressure of ozone was put in the reaction cell and then nitrous oxide was-added. Prior to irradiation the lamps were given 10 minutes to warm up to achieve constant intensity. After irradiation, the sample was passed through a liquid nitrogen trap to retain the unreacted condensibles. An aliquot of the non-condensables was then analyzed by means of gas chromatography.

It was found that good results could be obtained only if the vacuum and reaction cell were conditioned. This was done by occasionally leaving small amounts of ozone in the vacuum line overnight.

CHAPTER III

RESULTS

Photolysis at 2537 A

Mixtures of ozone and nitrous oxide at room temperature were photolyzed by 2537 A radiation. These mixtures were made by maintaining a constant ozone pressure and varying the nitrous oxide concentration; this was done for three separate ozone pressures. The experimental conditions for the photolysis at 2537 A are contained in Table 5 .

The only product measured was nitrogen; attempts to follow the ozone photodecomposition photometrically proved to be experimentally unfeasible. The nitrogen measured came from two sources, reaction 9a and a dark reaction. Since the dark reaction was dependent on several variables, a dark run was performed immediately following each photolysis to determine the nitrogen background. Correction for the dark reaction amounted to between zero to twenty percent of the total nitrogen yield.

Figure 4 shows the variation of the quantum yield of nitrogen at 2537 A as a function of the ratio $[N_2O]/[O_3]$. The quantum yield of nitrogen increases as the ratio of $[N_2O]/[O_3]$ increases until it reaches a maximum value of 0.37 ± 0.04, at which point the quantum yield of nitrogen remains constant. Within the limits of experimental uncertainty, the data fit the curve in Figure 4 for all three ozone pressures used at 2537 A.

In order to maintain the ratio of $[N_2O]/[O_3]$ reasonably constant throughout each run it was necessary to limit the conversion

TABLE 5

PHOTOLYSIS AT 2537 A

$O_3(t)$	$N_2O(t)$	Irradiation time (min)	$I_a (\mu / min)$	$N_2^*(\mu)$	$\Phi\{N_2\}$
0.910	57.0	15	1.28	8.2	.426
0.910	13.9	15	1.28	7.8	.405
0.875	8.8	15	1.28	8.25	.428
0.875	5.7	15	1.28	6.7	.348
0.910	2.2	15	1.28	3.5	.183
0.910	3.6	15	1.28	5.0	.260
0.910	235	15	1.28	7.5	.391
2.53	516	30	1.25	13.5	.360
2.53	110	30	1.25	13.7	.364
2.60	265	30	1.25	13.5	.360
2.60	31.2	30	1.25	9.1	.242
2.53	12.1	30	1.25	8.2	.218
2.53	4.2	30	1.25	4.6	.120
2.60	9.2	30	1.25	8.3	.221
2.50	45.2	30	1.25	12.5	.332
2.57	5.70	30	1.25	6.8	.181
2.60	27.0	30	1.25	12.2	.315
5.89	67.6	30	1.19	9.75	.273
5.83	7.3	30	1.19	4.45	.120
5.85	184	30	1.19	12.2	.345
5.78	25.0	30	1.19	8.3	.232
5.85	371	30	1.19	11.7	.328

TABLE 5 cont'd

PHOTOLYSIS AT 2537 A

$O_3(t)$	$N_2O(t)$	Irradiation time (min)	$I_a(\mu/min)$	$N_2^*(\mu)$	$\Phi\{N_2\}$
5.86	527	30	1.19	10.5	.290
5.88	180	30	1.19	12.6	.353
5.86	282	30	1.19	12.8	.358

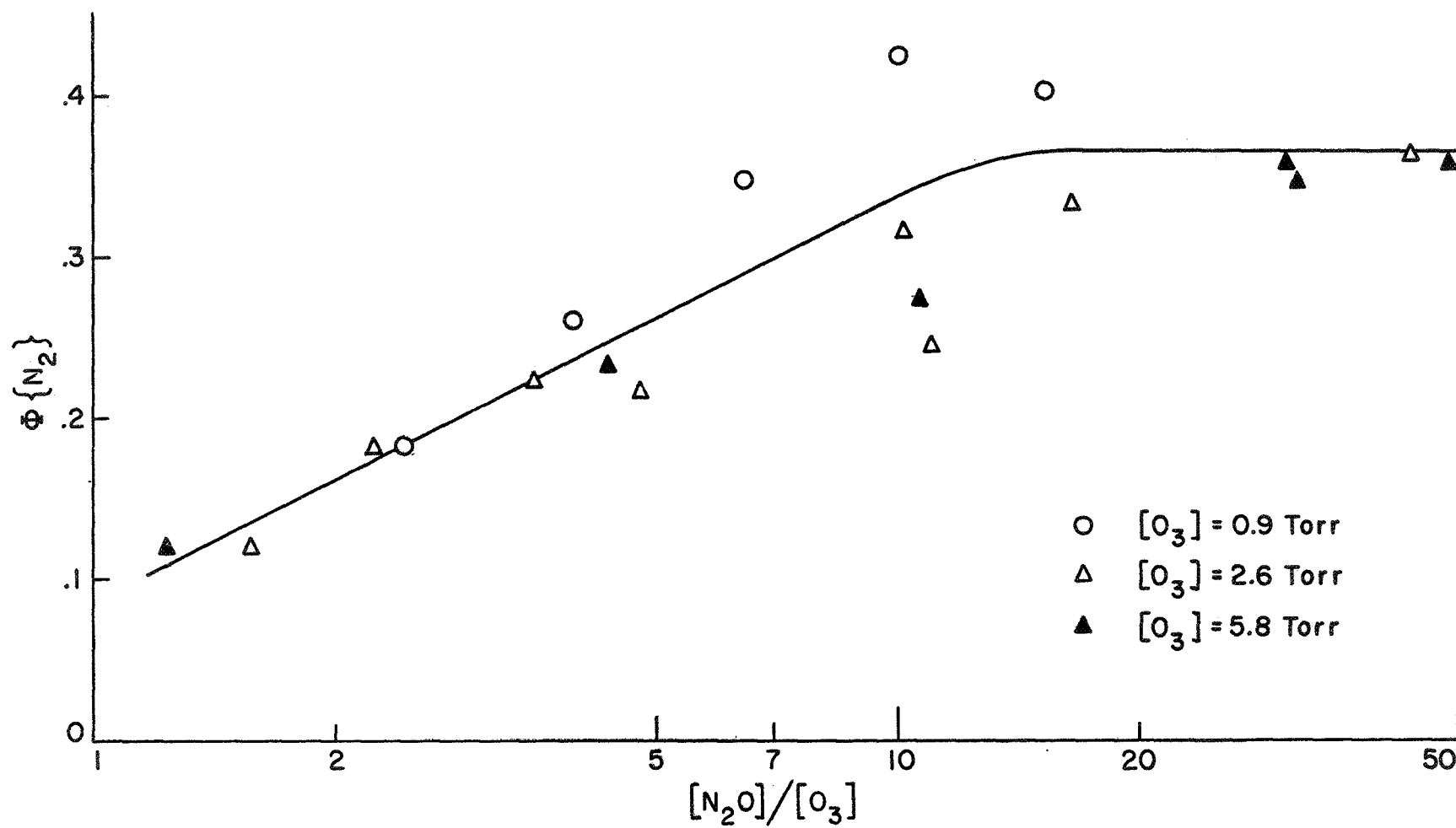* Corrected for background and dark reaction.

FIGURE 4

$\Phi \{N_2\}$ AS A FUNCTION OF $[N_2O]/[O_3]$ AT 2537 A

of the reaction mixtures. The maximum amount of ozone decomposed was always less than fifteen percent of the initial concentration. In maintaining this limit-it was necessary to take into account that the ozone in the cell also reacted with the NO formed in reaction 9b. In this work it was found that each NO molecule formed removed between one and one half to three ozone molecules in the course of a run.

Photolysis at 2288 A

The conditions and results of the radiation of ozone-nitrous oxide mixtures at 2288 A are contained in Table 6. At this wave-length only one ozone pressure was used (0.9 torr), as it had been determined previously at 2537 A that the quantum yield of nitrogen was dependent on the ratio and not the absolute amount of ozone in the reaction vessel.

The effect of intensity was studied at 2288 A by varying the intensity by a factor of nine. The results of this work are shown in Figure 5. At low $[N_2O]/[O_3]$ ratios there was no effect, however at high N_2O pressures there was an increase in the amount of nitrogen obtained. This increase in nitrogen, however, was found to be taking place through reaction 7, the direct photolysis of nitrous oxide, rather than due to any intensity effect. This photolysis was the result of removing a filter to increase the intensity, allowing some lower wavelength radiation to enter the cell.

The behavior of the increase in nitrogen yield at 2288 A as the ratio $[N_2O]/[O_3]$ increased was the same as that observed at 2537 A. However, the value of $\Phi\{N_2\}$ where the 2537 A radiation

TABLE 6

PHOTOLYSIS AT 2288 A[**]

$O_3(t)$	$N_2O(t)$	Irradiation time (min)	$I_a(\mu/min)$	$N_2{}^*(\mu)$	$\Phi\{N_2\}$
.910	16.4	30	1.18	12.2	.345
.910	48.5	30	1.18	12.1	.343
.930	113	30	1.18	11.7	.331
.890	2.0	30	1.18	3.3	.093
.875	4.9	30	1.18	5.3	.150
.885	8.0	30	1.18	10	.282
.910	2.4	30	0.95	3.3	.115
.910	3.20	30	0.95	4.4	.154
.910	6.35	30	0.95	6.1	.215
.875	3.6	4.6	8.58	8.9	.230
.890	5.5	5.0	8.58	12.15	.284
.875	18.6	5.0	8.58	13.3	.312
.875	105	5.0	8.58	23.0	.536
.890	29.1	30	0.95	9.9	.347

* Corrected for background and dark reaction.
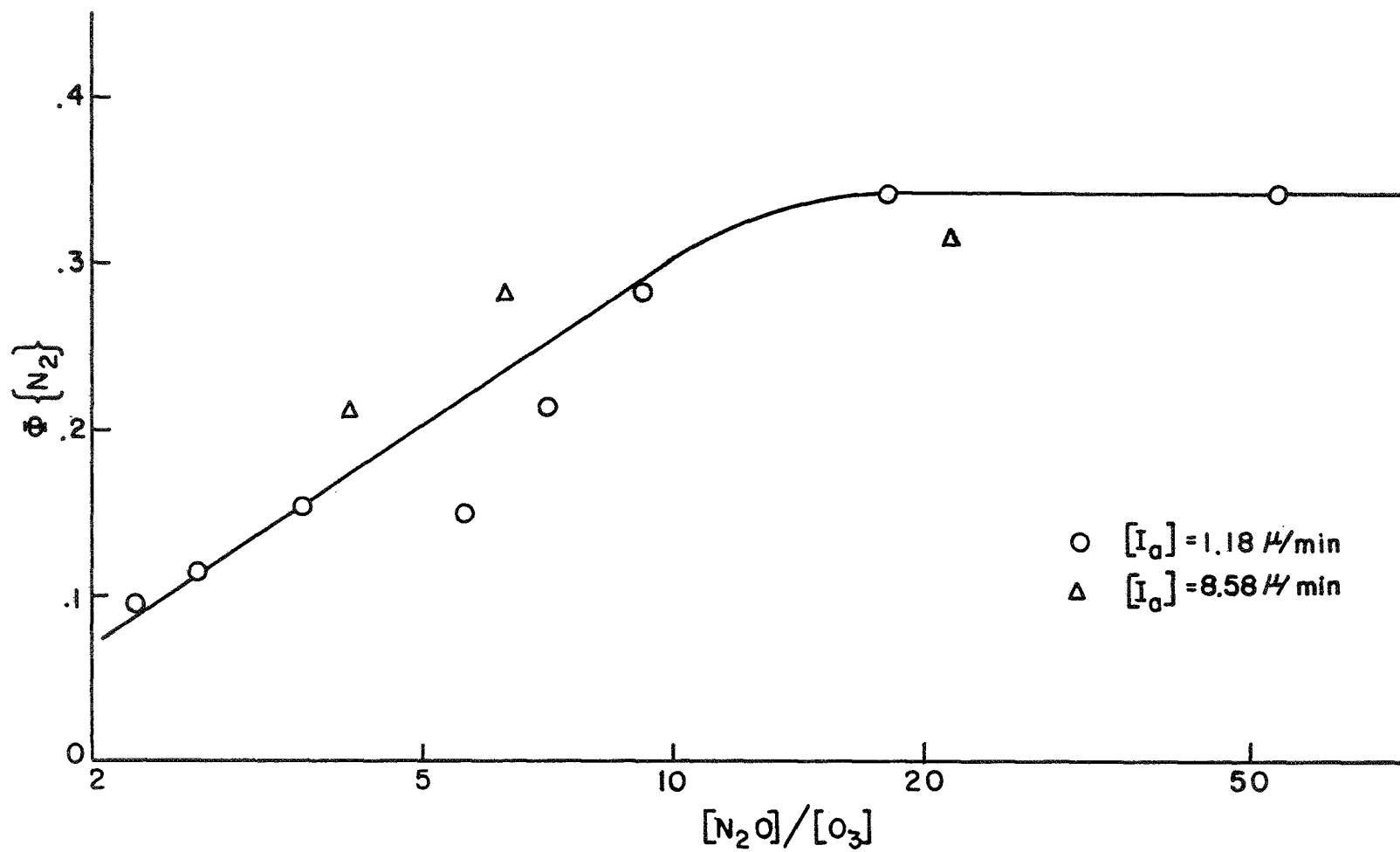**All runs done ar room temperature.

FIGURE 5

$\Phi \{N_2\}$ AS A FUNCTION OF $[N_2O]/[O_3]$ AT 2288 A

leveled off was $0.37 \pm .04$, whereas the maximum value for $\Phi\{N_2\}$ at 2288 A was $0.345 \pm .04$. This slightly lower value for $\Phi\{N_2\}$ at 2288 A could be either real or due to experimental error.

Foreign Gas Effects

When ozone is photolyzed at 2537 A and at 2288 A, there is a substantial amount of energy available in excess of that needed for dissociation. Part of this excess energy goes into the translational energy of the $O(^1D)$ atom formed from the photodissociation of the ozone. To study whether this excess energy had any effect on the rates of the reaction being studied, a foreign gas was added to the mixtures of nitrous oxide and ozone for the purpose of removing this excess translational energy. Helium was chosen as the foreign gas because it only removed translational energy and did not quench the $O(^1D)$ atom to its $O(^3P)$ ground state.[26] The results of the helium addition are shown in Table 7.

The effect of adding helium was studied at both wavelengths, as a function of the ratio $[N_2O]/[O_3]$, and as a function of helium pressure. The results of varying the helium pressure are shown in Figure 6. In Figure 6 the experimental condition chosen was one where nearly all the $O(^1D)$ formed in the photolysis of ozone was reacting with the nitrous oxide (reaction 9). At this condition the quantum yield of nitrogen formation was approximately equal to k_{9a}/k_9. The curve indicates that this ratio increases as helium removes the excess translational energy from the $O(^1D)$ atom.

The effect on the quantum yield of nitrogen of varying the ratio $[N_2O]/[O_3]$ in the presence of an excess of helium is shown

TABLE 7

EFFECT OF HELIUM

$O_3(t)$	$N_2O(t)$	He(t)	Irradiation time (min)	$I_a(\mu/min)$	$N_2^*(\mu)$	$\Phi\{N_2\}$	λ (A)
.89	29.1	0.0	30	0.95	9.9	.347	2288
.89	29.1	150	30	0.95	16.5	.578	2288
.875	28.7	690	30.5	0.95	20.6	.720	2288
.91	29.0	710	30	0.95	21.7	.76	2288
.875	30.0	65	30	0.95	19.4	.68	2288
.89	28.6	60	30	0.95	17.2	.60	2288
.89	29.1	170	32	0.95	16.7	.553	2288
.910	28.7	385	30	0.95	20.8	.730	2288
.910	28.7	385	30	0.95	20.8	.730	2288
.89	6.2	380	30	0.95	11.0	.384	2288
.86	3.35	415	30	0.95	9.2	.321	2288
.91	1.3	390	30	1.044	6.9	.220	2288
.875	10.5	365	32.5	1.044	18.6		2288
.875	60.0	410	30	1.044	19.2	.613	2288
.910	3.42	360	30	1.044	16.8	.536	2288
.875	2.3	360	30.5	1.044	8.5	.298	2288
.89	1.88	370	30	1.044	14.3	.456	2288
.89	2.3	212	30	1.044	14.3	.456	2288
.91	1.45	400	30	1.044	8.15	.286	2288
.897	7.05	400	20	1.28	17.2	.670	2537
.910	28.25	400	30	1.28	33.55	.873	2537

TABLE 7 cont'd

EFFECT OF HELIUM

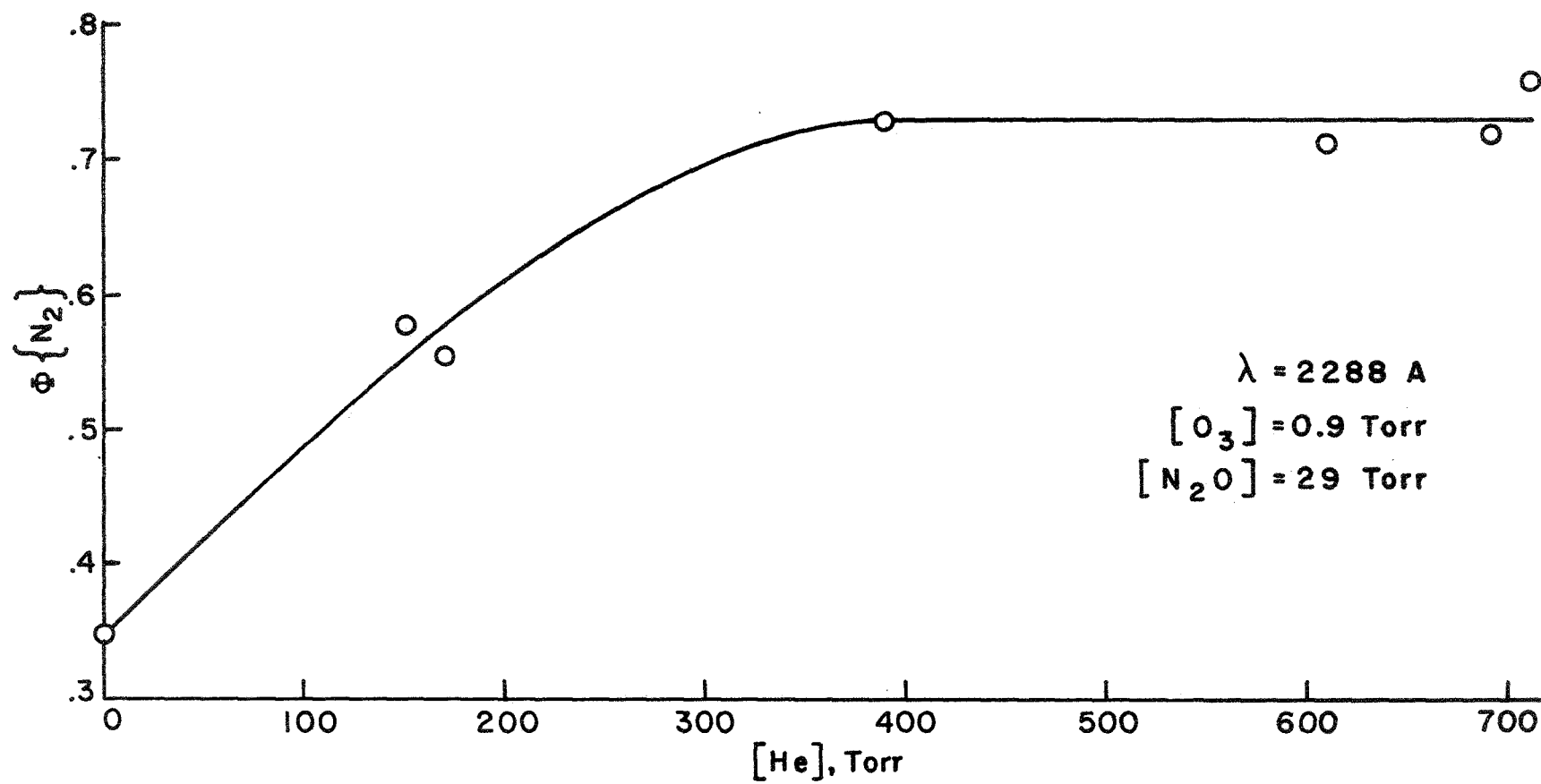| $O_3(t)$	$N_2O(t)$	He(t)	Irradiation time (min)	$Ia(\mu/min)$	$N_2^*(\mu)$	$\Phi\{N_2\}$	$\lambda(A)$
.877	3.1	450	20	1.28	13.8	.539	2537
.910	1.45	420	21	1.28	10.0	.371	2537
.89	4.85	450	20	1.28	16.8	.656	2537

* Corrected for background and dark reactions

FIGURE 6

THE EFFECT OF ADDING HELIUM, VARYING HELIUM PRESSURE

in Figure 7. It can be seen that the quantum yield of nitrogen is greater at every point when compared to the results shown in Figures 4 and 5 where helium is not present as a foreign gas.
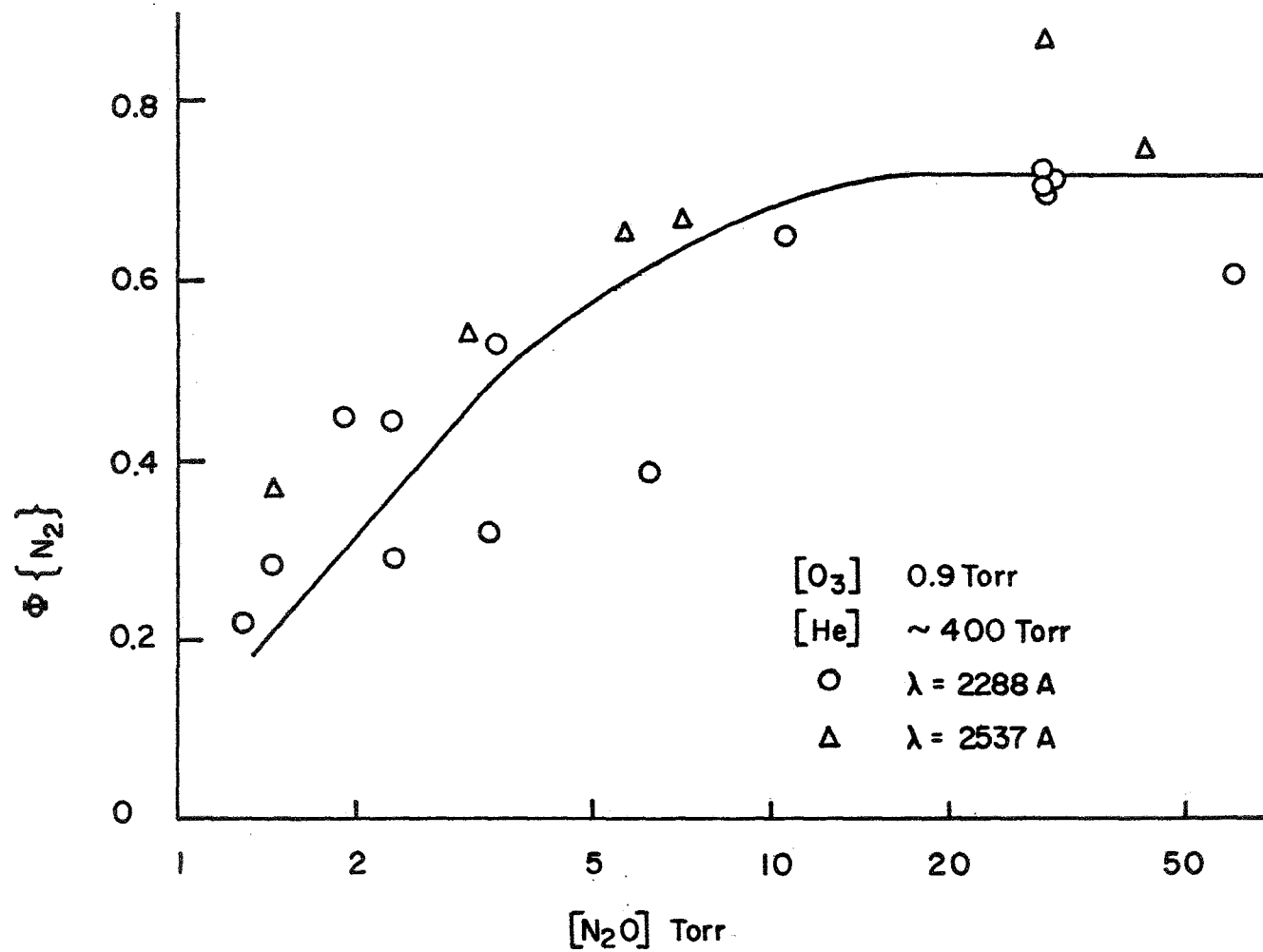
FIGURE 7

THE EFFECT OF ADDING HELIUM,
VARYING NITROUS OXIDE PRESSURE

CHAPTER IV

DISCUSSION

Analysis of Results in the Absence of Helium

To analyze the results the following mechanism is proposed.

$$O_3 + h\nu \rightarrow O_2^* + O(^1D) \qquad\qquad 1$$

$$O(^1D) + O_3 \rightarrow O_2 + O_2^\dagger \qquad\qquad 2$$

$$O_2^\dagger + O_3 \rightarrow 2O_2 + O(^1D) \qquad\qquad 3$$

$$O_2^* + O_3 \rightarrow 2O_2 + O(^3P) \qquad\qquad 4$$

$$O(^3P) + O_3 \rightarrow 2O_2 \qquad\qquad 5$$

$$O(^1D) + N_2O \rightarrow N_2 + O_2 \qquad\qquad 9a$$

$$\rightarrow 2NO \qquad\qquad 9b$$

$$O_2^* + N_2O \rightarrow N_2 + O_3 \qquad\qquad 10a$$

$$\rightarrow N_2O + O_2 \qquad\qquad 10b$$

$$O_2^\dagger + N_2O \rightarrow N_2 + O_3 \qquad\qquad 11a$$

$$\rightarrow N_2O + O_2 \qquad\qquad 11b$$

The expression for the quantum yield of nitrogen is given by the equation

$$\Phi\{N_2\} = \frac{k_{9a}(k_3[O_3] + k_{11}[N_2O]) + k_{11a}k_2[O_3]}{k_9(k_3[O_3] + k_{11}[N_2O]) + k_{11}k_2[O_3]} + \frac{k_{10a}[N_2O]}{k_4[O_3] + k_{10}[N_2O]} \; .$$

As the ratio $[N_2O]/[O_3] \rightarrow \infty$, the limiting expression for the quantum yield of nitrogen, $\Phi_\infty\{N_2\}$, is given by

$$\Phi_\infty\{N_2\} = \frac{k_{10a}}{k_{10}} + \frac{k_{9a}}{k_9} \; .$$

At high $[N_2O]/[O_3]$ ratios we find the quantum yield of nitrogen to be equal to 0.37, which is the lowest value reported for the ratio k_{9a}/k_9 by other researchers. Therefore, it can be assumed that reaction 10a, the formation of nitrogen by the reaction of O_2^* with nitrous oxide, is negligible compared to reaction 9a.

At low ratios of $[N_2O]/[O_3]$, the limiting expression for the quantum yield of nitrogen, $\Phi_o\{N_2\}$ is given by

$$\Phi_o\{N_2\} = \frac{k_3 \, k_{9a} + k_2 \, k_{11a}}{k_3 \, k_9 + k_2 \, k_{11}} \; .$$

It was shown in Figures 4 and 5 that $\Phi\{N_2\}$ approaches zero as the ratio $[O_3]/[N_2O]$ approaches zero; in order for the above expression to conform with this experimental result $k_{11} \gg k_{11a}$. It therefore follows that the only reaction important in the formation of nitrogen is reaction 9a, the reaction of $O(^1D)$ with nitrous oxide.

The $O(^1D)$ can come from the photolysis of ozone or from the reaction of $O_2^\dagger$ with ozone, reaction 3. Since the $O(^1D)$ from both sources can react to form nitrogen, the mechanism predicts that

$$\left[\Phi\{N_2\}^{-1} - \frac{k_9}{k_{9a}} \right]^{-1} = \frac{k_{9a} \, [N_2O]}{k_2 \, [O_3]} + \frac{k_3 \, k_{9a}}{k_{10} \, k_2} \; .$$

When $[\Phi\{N_2\}^{-1} - k_9/k_{9a}]^{-1}$ is plotted versus the ratio $[N_2O]/[O_3]$, the intercept of the line plotted is equal to $(k_3/k_{10})(k_{9a}/k_2)$, and the slope is equal to (K_{9a}/k_2). This is shown in Figure 8 for the runs at 2537 A and in Figure 9 for the runs at 2288 A. The intercept of both these graphs is approximately equal to zero, therefore k_{10} must be much greater than k_3. This indicates that almost all the $O(^1D)$ produced came from reaction 1 and hence the quantum yield for $O(^1D)$ formation is equal to unity.[25]

The $O(^1D)$ formed can react with either of the two constituents of the reaction mixture, ozone or nitrous oxide. Rate constants for both cases have been recorded in the literature and are shown in Table 8.

TABLE 8

RATE CONSTANTS FOR REACTION OF $O(^1D)$ WITH
OZONE AND NITROUS OXIDE

Reaction	Rate Constant $M^{-1} sec^{-1}$	Ref.
$O(^1D) + O_3 \rightarrow 2O_2$	$k_2 = 4.0 \pm 0.5 \times 10^{10}$	26
	$2.0 \pm 1.0 \times 10^{11}$	27
$O(^1D) + N_2O \rightarrow$ Prods.	$k_9 = 1.1 \times 10^{11}$	28

These rate constants leave considerable doubt about the ratio k_2/k_9. This work, while not able to determine the absolute rates of k_2 and k_9, has been able to determine the relative ratio k_2/k_9. This was done using the following simplified mechanism composed of the steps shown to be important in the system studied.
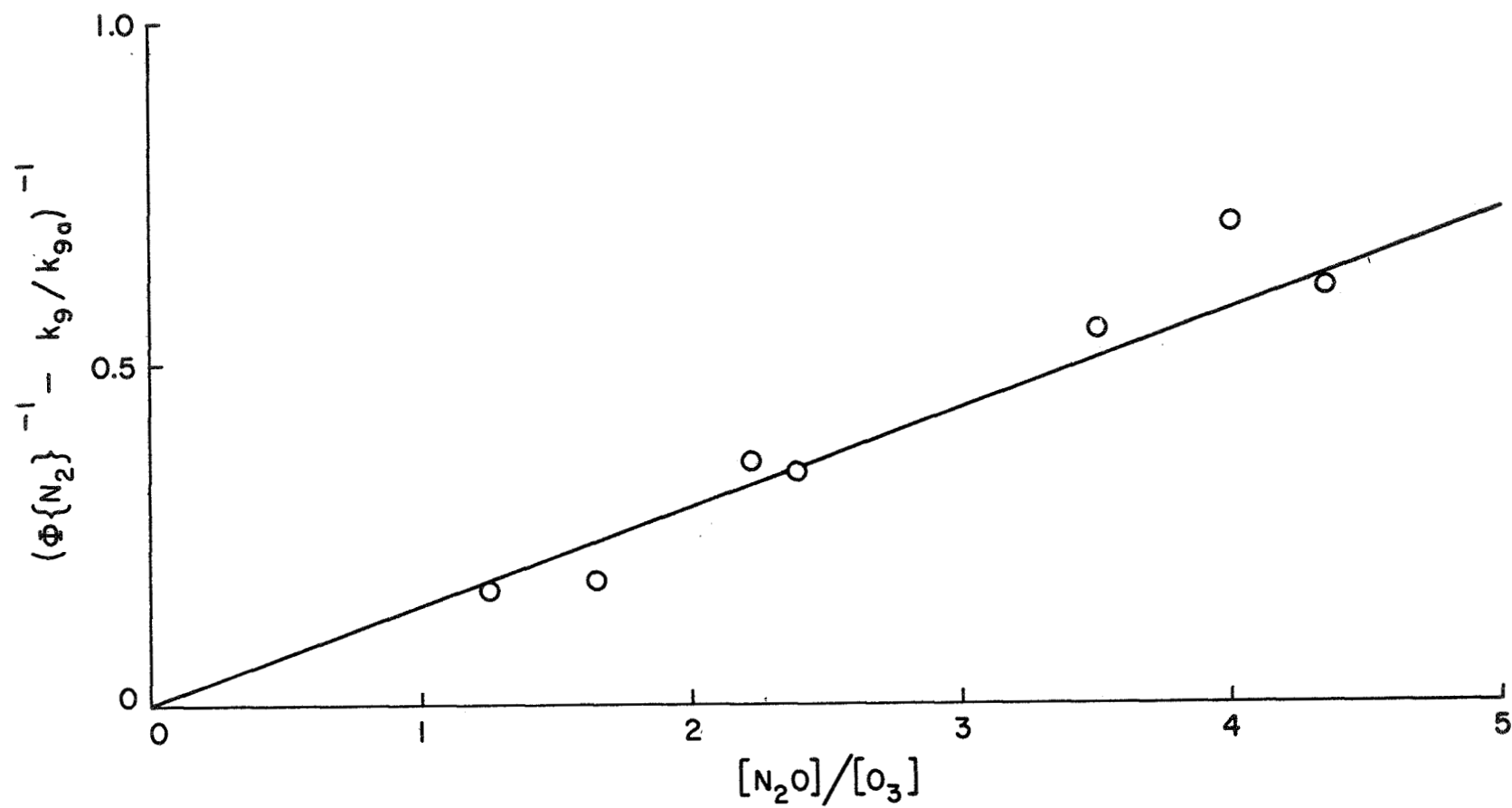
FIGURE 8

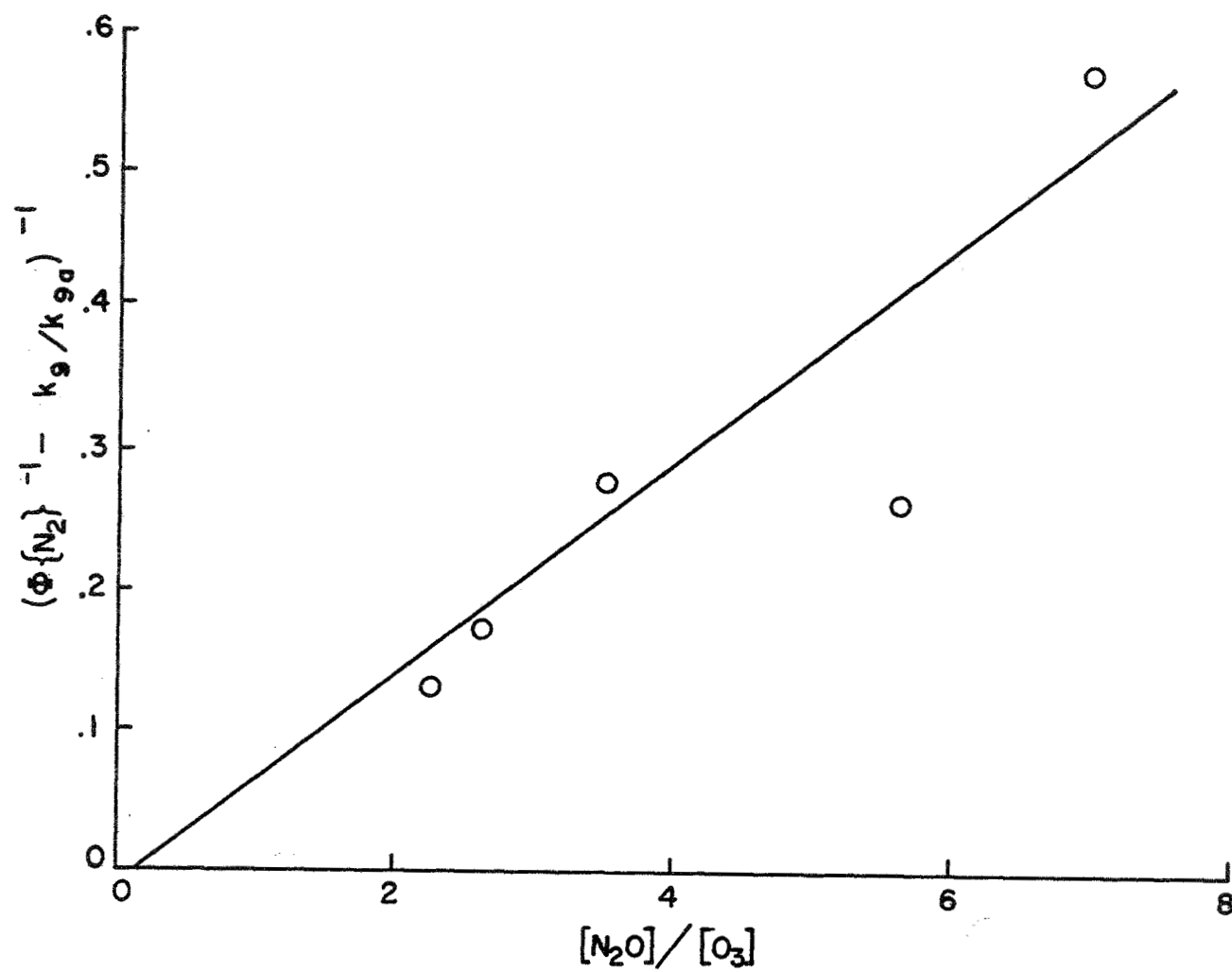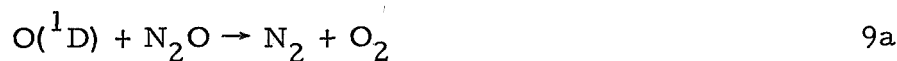$(\Phi\{N_2\}^{-1}-k_9/k_{9a})^{-1}$ AS A FUNCTION OF $[N_2O]/[O_3]$ AT 2537 A
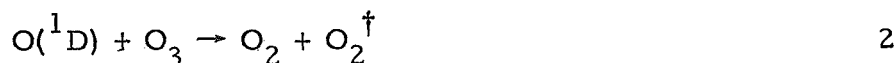
FIGURE 9

$(\Phi\{N_2\}^{-1} - k_9/k_{9a})^{-1}$ AS A FUNCTION OF $[N_2O]/[O_3]$ AT 2288 A

$$O_3 + h\nu \rightarrow O_2^* + O(^1D) \qquad\qquad 1$$

$$O(^1D) + O_3 \rightarrow O_2 + O_2^\dagger \qquad\qquad 2$$

$$O(^1D) + N_2O \rightarrow N_2 + O_2 \qquad\qquad 9a$$

$$\rightarrow 2NO \qquad\qquad 9b$$

$$O_2^* + N_2O \rightarrow O_2 + N_2O \qquad\qquad 10b$$

$$O_2^\dagger + N_2O \rightarrow O_2 + N_2O \qquad\qquad 11b$$

This mechanism predicts the following expression,

$$\Phi\{N_2\}^{-1} = (k_9/k_{9a}) + (k_2/k_{9a})\,([O_3]/[N_2O]).$$

A plot of $\Phi\{N_2\}^{-1}$ as a function of the ratio $[O_3]/[N_2O]$ has a slope corresponding to the value (k_2/k_{9a}) and an intercept equal to the ratio (k_9/k_{9a}). This has been plotted in Figure 10 for the data at 2537 A in the absence of helium and in Figure 11 for the data at 2288 A in the absence of helium. The values for k_2/k_9 and k_{9a}/k_{9b} obtained from these plots are listed in Tables 9 and 10.

These results indicate that $O(^1D)$ reacts faster with ozone than it does with nitrous oxide. Also indicated is a wavelength effect. At the higher energy due to 2288 A radiation the reaction of $O(^1D)$ with ozone is even more highly favored. Figures 4 and 5 show this competition between ozone and nitrous oxide at low N_2O pressures.

At the high end of the curves shown in Figures 4 and 5, all the $O(^1D)$ is reacting with nitrous oxide; the addition of more nitrous
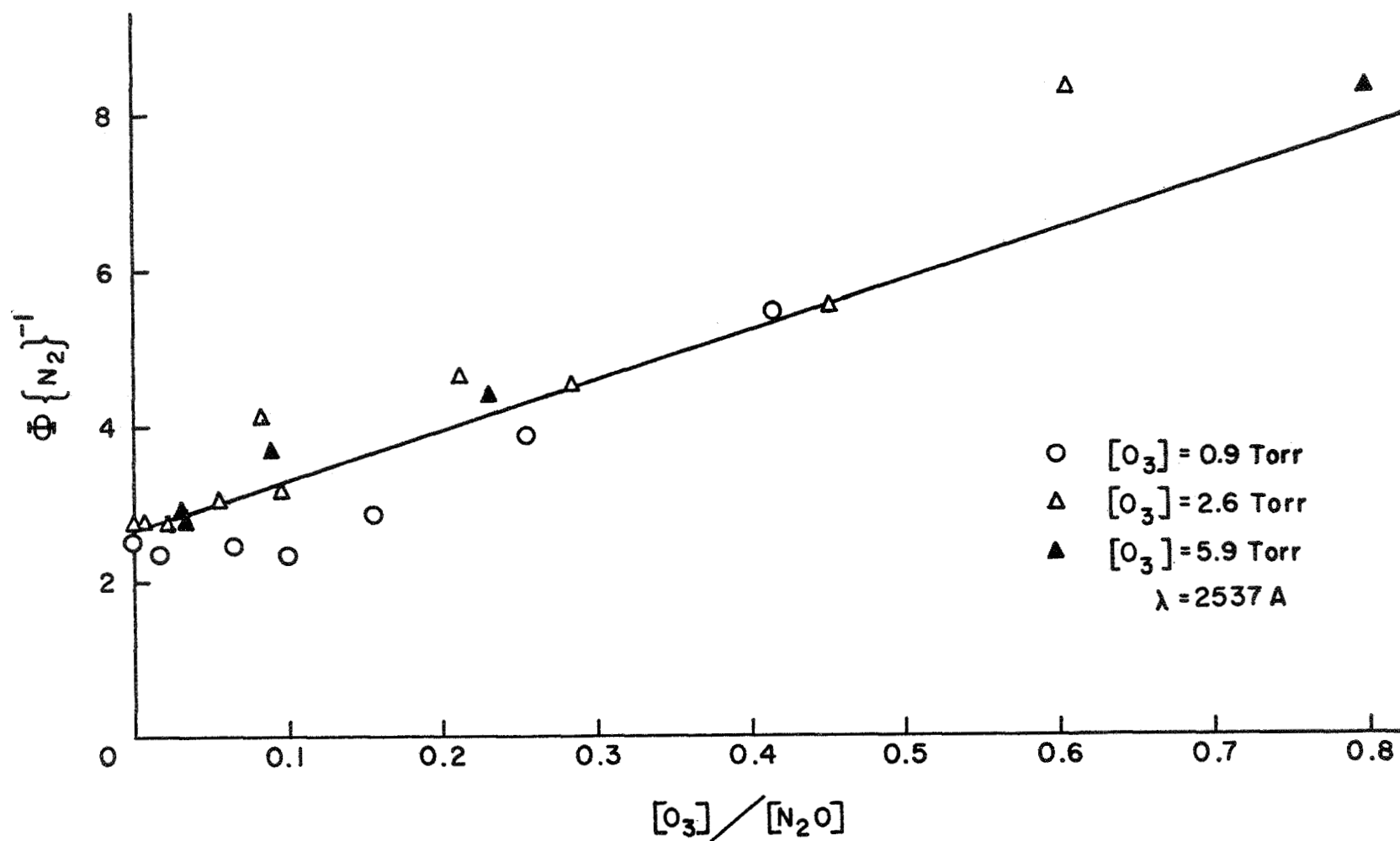
FIGURE 10

$\Phi\{N_2\}^{-1}$ AS A FUNCTION OF $[O_3]/[N_2O]$ AT
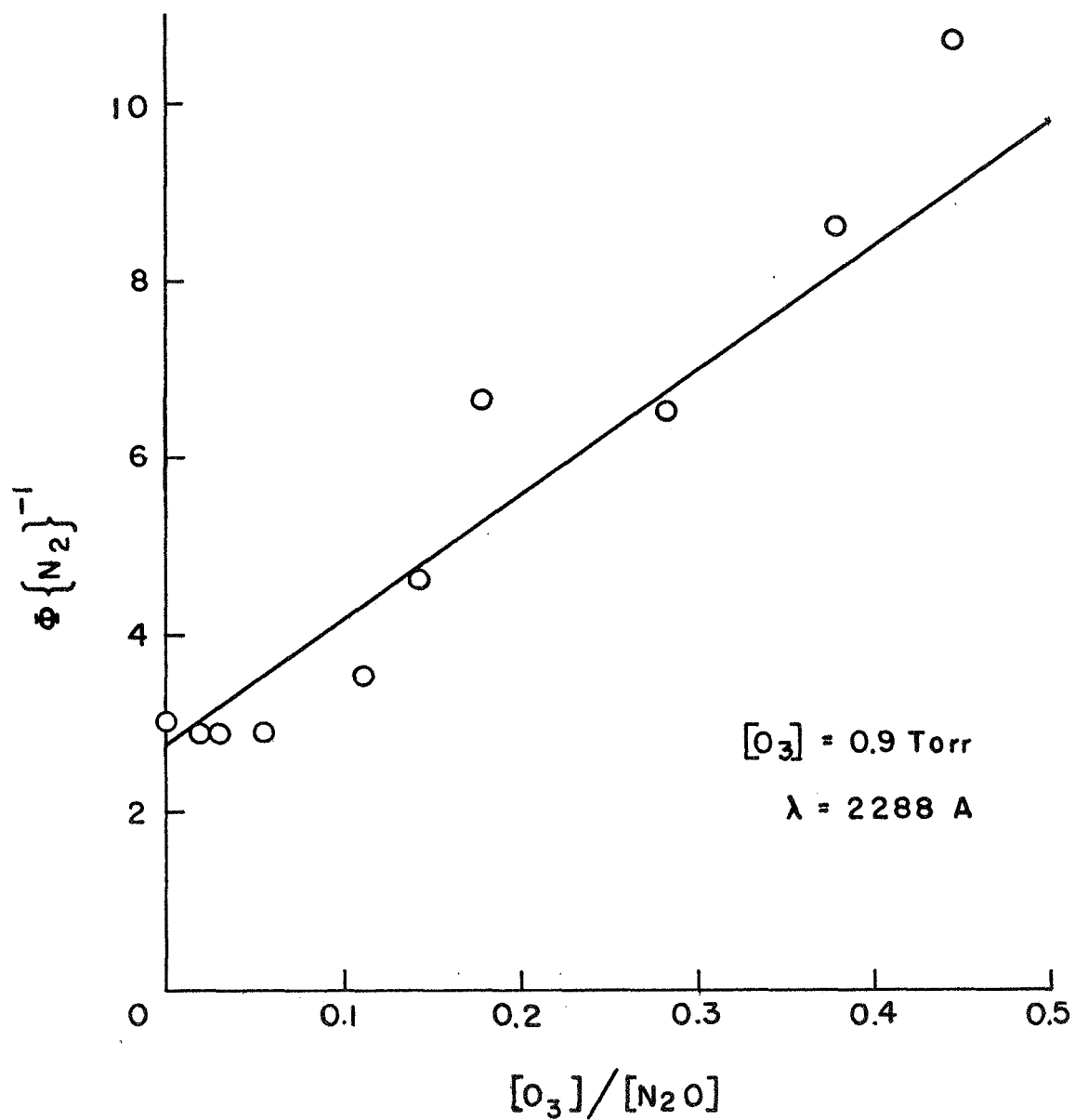2537 A WITH NO HELIUM PRESENT

FIGURE 11

$\Phi \{N_2\}^{-1}$ AS A FUNCTION OF $[O_3]/[N_2O]$ AT
2288 A WITH NO HELIUM PRESENT

TABLE 9

RELATIVE RATE CONSTANTS

Ratio	Relative Rate	Wavelength A	[He], torr
k_2/k_9	6.85	2288	0
k_2/k_9	2.63	2537	0
k_2/k_9	2.13	2288	400
k_2/k_9	2.27	2537	400

oxide to these mixtures has no further effect in increasing the

nitrogen quantum yield. At these conditions the competition between

reactions 9a and 9b can be studied. This competition has been studied

by many researchers before, and the results obtained have had

considerable differences. A listing of some of these results and

the conditions at which the $O(^1D)$ was generated are shown in Table 10.

In this work the value of k_{9a}/k_{9b} was obtained in two ways.

One way for obtaining this value was from the intercept of the lines

in Figures 10 and 11. The other way in which the value of k_{9a}/k_{9b}

is obtained is that at high $[N_2O]/[O_3]$ ratios the quantum yield of

nitrogen is equal to the ratio k_{9a}/k_9.

Foreign Gas Effects

The values obtained for the ratio k_{9a}/k_{9b} when no foreign

gas was present agreed with previous work done in this laboratory.[23]

However, with the addition of helium as a foreign gas, the ratio

k_{9a}/k_{9b} became considerably greater. This is shown in Figure 12;

the value of the intercepts decrease in the presence of helium.

TABLE 10

VALUES OF k_{9a}/k_{9b}

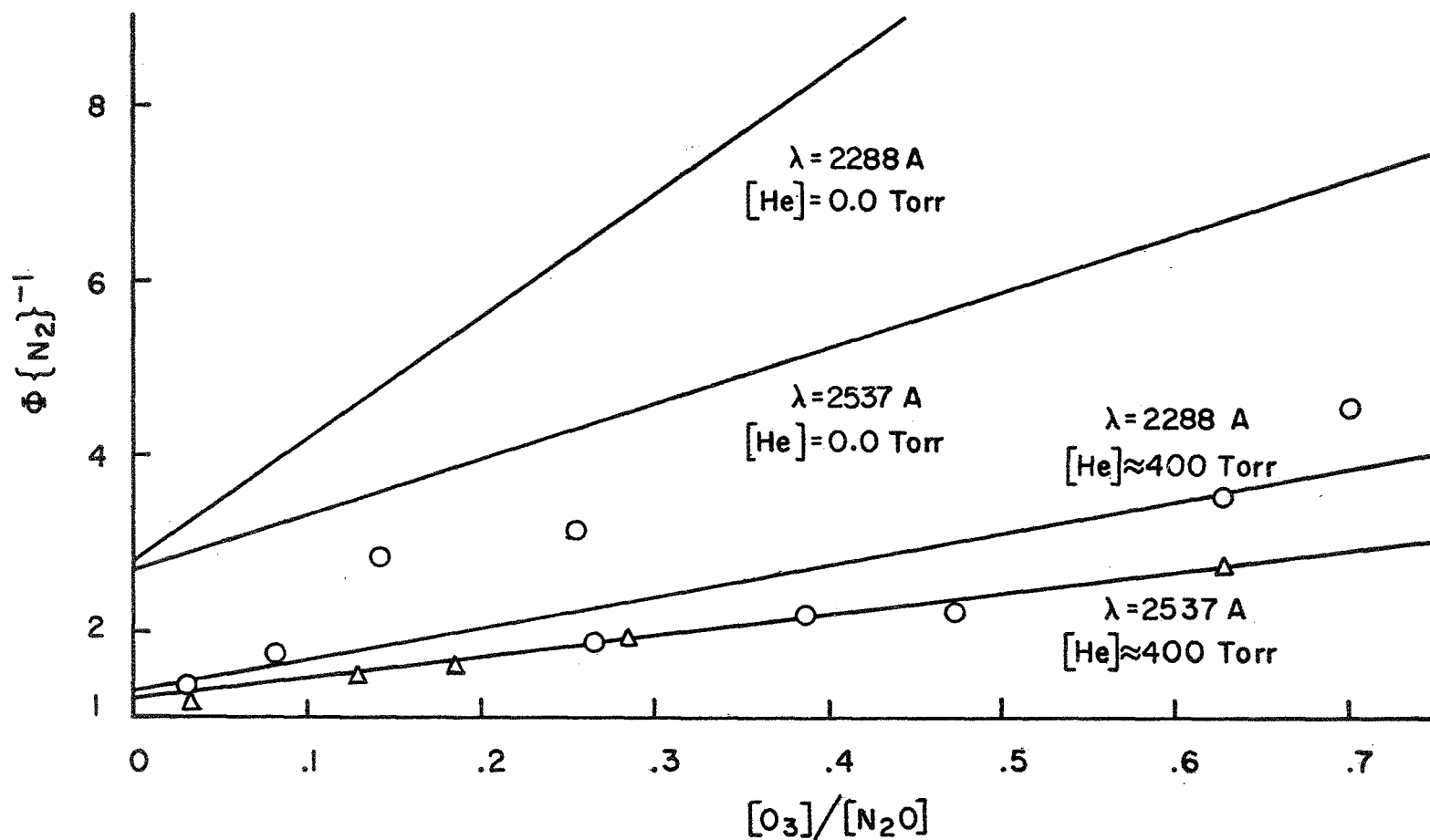| Value	Source of $O(^1D)$	Ref.
1.0	Photolysis N_2O, 1850-1950 A	29
0.7	Photolysis N_2O, 1850-1950 A	15
1.05	Photolysis NO_2, 2288 A	30
1.56	Photolysis N_2O 1849 A	31
0.59	Photolysis N_2O, 2139 A	23
0.53	Photolysis O_3, 2288 A	this work
0.59	Photolysis O_3, 2537 A	this work
2.55	Photolysis O_3, 2288 A with He added	this work
4.0 ± 2.0	Photolysis O_3, 2537 A with He added	this work

FIGURE 12

$\Phi\{N_2\}^{-1}$ AS A FUNCTION OF $[O_3]/[N_2O]$
WITH HELIUM PRESENT

When helium was added as a foreign gas to mixtures of ozone and nitrous oxide being photolyzed at 2288 A, the ratio of k_2/k_9 decreased from 6.85 to 2.13. This lower value is, within the experimental uncertainty, the same value that is obtained for the photolysis of the mixtures at 2537 A.

The explanation for these phenomena appears to be the ability of helium to remove excess translational energy from the $O(^1D)$ atom without quenching it to the $O(^3P)$ ground state. This excess translational energy that the $O(^1D)$ atom possesses is due to the excess energy available in most of the common ways in which the $O(^1D)$ is prepared in the laboratory. Some common sources of $O(^1D)$ and the excess energy available after bond breaking and electronic excitation is shown in Table 11.

TABLE 11

SOURCES AND EXCESS ENERGY AVAILABLE

Sources	λ	E, kcal/mole
$N_2O + h\nu \rightarrow N_2 + O(^1D)$	2139 A	48.1
$O_3 + h\nu \rightarrow O_2(^1\Delta) + O(^1D)$	2288 A	31.8
$O_3 + h\nu \rightarrow O_2(^1\Delta) + O(^1D)$	2537 A	20.3
$NO_2 + h\nu \rightarrow NO + O(^1D)$	2288 A	5.6

This excess energy is distributed between the $O(^1D)$ atom and the remaining molecular fragment. The $O(^1D)$ picks up its share of the excess energy in the form of excess translational energy. The molecules of either N_2, NO, or O_2 depending on which source of $O(^1D)$

is used, can distribute their share of the excess energy in the form of excess translational, vibrational and/or rotational energy.

In the present investigation, due to the structures of the molecules from which the $O(^1D)$ was produced, we assume that the excess energy available was distributed evenly between the $O(^1D)$ atom and the fragment molecule. It is this excess translational energy of the $O(^1D)$ that the addition of helium as a foreign gas removes as a consequence of collisions between the $O(^1D)$ atom and the helium in the reaction mixtures.

With the hard sphere model for atomic collisions, the average amount of translational energy removed from the $O(^1D)$ atom after a collision with helium is given by the equation[34]

$$\frac{E_T{}'}{E_T} = \frac{\int_0^\pi (M_{O(^1D)}{}^2 + M_{He}{}^2 + 2M_{O(^1D)}M_{He} \cos\theta_r) \sin\theta_r d\theta_r}{\int_0^\pi \sin\theta_r d\theta_r}$$

where E_T is the excess translational energy before collision, $E_T{}'$ is the excess translational energy after collision, θ_r is the relative scattering angle of the $O(^1D)$ atom after collision, and M is the mass of the respective atoms. Upon integration this expression reduces to the form:

$$\frac{E_T{}'}{E_T} = \frac{M_{O(^1D)}{}^2 + M_{He}{}^2}{(M_{O(^1D)} + M_{He})^2}$$

Therefore, assuming a completely elastic collision, an average of 32 percent of the translational energy before collision

is removed. The dissipation of the excess translational energy of the $O(^1D)$ atom as a function of the number of collisions with helium is shown in Figure 13.

In the presence of helium in the reaction mixture, the $O(^1D)$ atoms will have some of their excess translational energy removed by collision with helium atoms. The number of times that an average $O(^1D)$ atom will collide with a helium atom before colliding with a nitrous oxide molecule is given by the ratio

$$\sigma^2_{N_2O-O}[He]/\sigma^2_{He-O}[N_2O]$$

where $\sigma^2_{N_2O-O}$ and σ^2_{He-O} are the collision cross section of the $O(^1D)$ atom with nitrous oxide and helium respectively. Table 12 contains the values of σ ($\sigma^2_{1-2} = (\frac{\sigma_1 + \sigma_2}{2})^2$) for the various species of interest.

TABLE 12

VALUES OF σ^a

Species	σ, A	Ref.
$O(^1D)^b$	2.9	33
N_2O	4.71	32
He	2.18	32

a. from viscosity data
b. value of $O(^1D)$ assumed to be same as for $O(^3P)$

From the values given in Table 12, the average number of collisions of an $O(^1D)$ atom with helium before colliding with a nitrous oxide molecule is calculated to be equal to $[He]/2.35[N_2O]$.
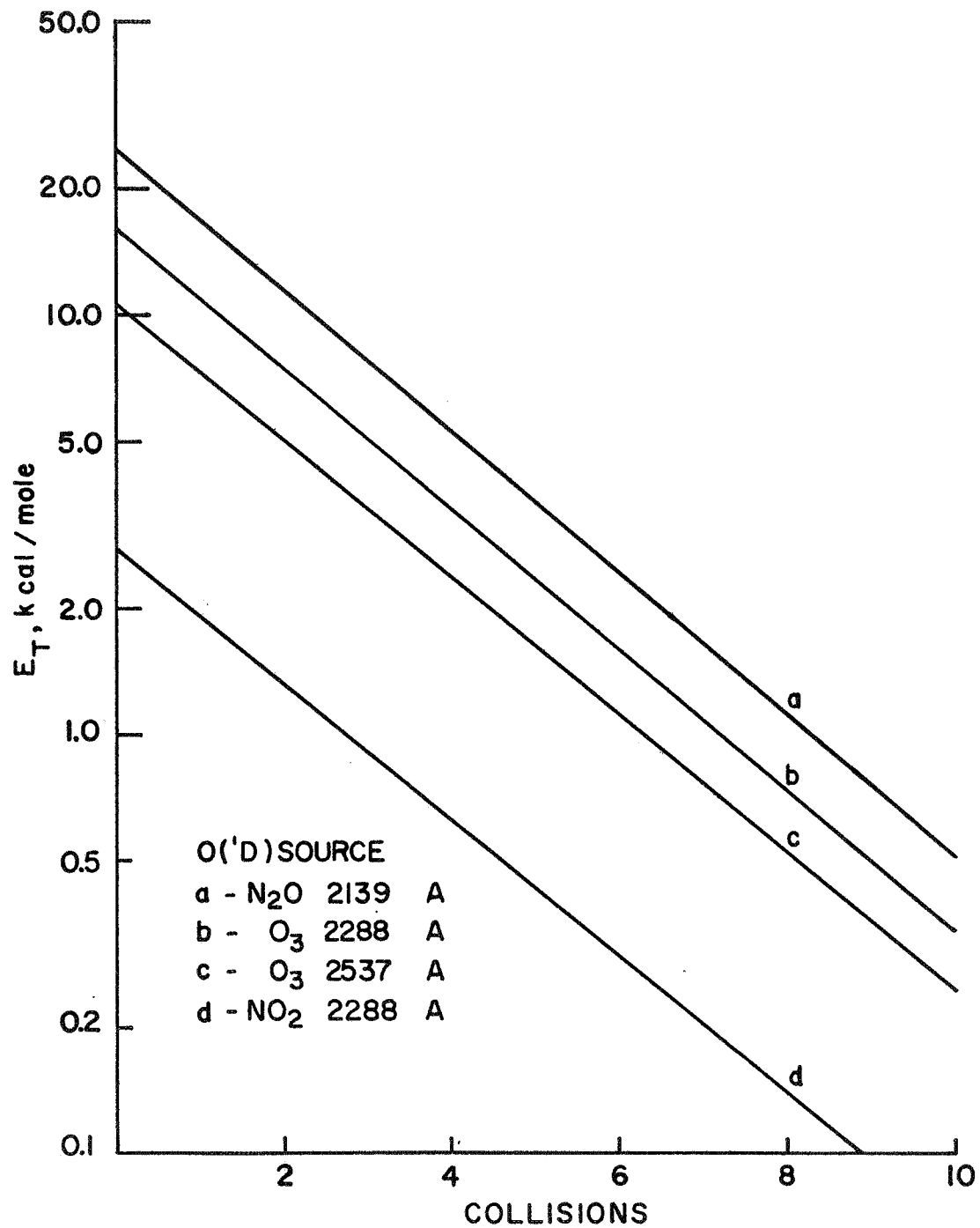
FIGURE 13

THE LOSS OF TRANSLATIONAL ENERGY BY COLLISION

However, since not every collision of an $O(^1D)$ atom with a nitrous oxide molecule results in a reaction, the number of times that an $O(^1D)$ atom collides with a helium atom before reacting is several times larger than $[He]/2.35 [N_2O]$.

At high helium pressures the $O(^1D)$ atom will have most of its excess translational energy removed by collisions. This means that the values of k_2/k_9 and k_{9a}/k_{9b} obtained in the presence of a large excess of helium are the values for the reaction of a "cold" $O(^1D)$ atom. A "cold" $O(^1D)$ atom possesses only electronic energy and thermally induced translational energy. The values of k_2/k_9 and k_{9a}/k_{9b} have been shown to be dependent on the amount of translational energy of the $O(^1D)$ atom.

In Figure 14 computed curves of k_{9a}/k_9 as a function of the amount of excess translational energy of the $O(^1D)$ atom are plotted. Curve 1 is plotted for the case of a reaction taking place every time an $O(^1D)$ atom collides with N_2O. Curves 2, 3, 4 are plotted for the cases of a reaction taking place between $O(^1D)$ and nitrous oxide on only 1/2, 1/3, or 1/4 of all their collisions with each other, respectively. To plot these curves, it was assumed that each collision of the $O(^1D)$ with helium was an elastic collision and hence 32 percent of the excess translational energy is removed by each collision as shown in Figure 12. From the values for the collision cross sections and assuming the average percentage of collisions between $O(^1D)$ and nitrous oxide resulting in reaction, the number of deactivating collisions between $O(^1D)$ and helium that take place prior to the $O(^1D)$ reacting with nitrous oxide can be calculated for any $[He]/[N_2O]$ ratio. Using the values of k_{9a}/k_9 found for varying $[He]/[N_2O]$
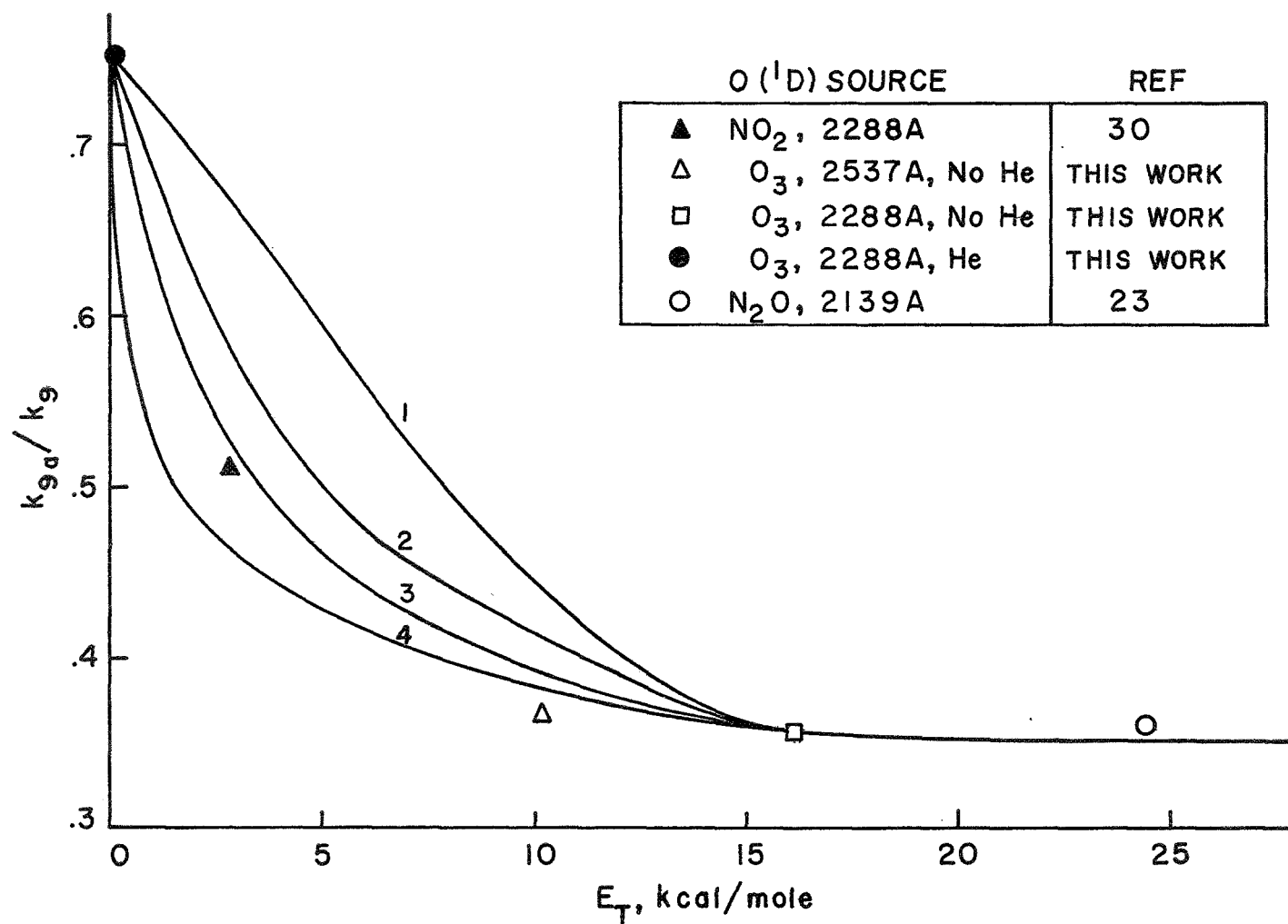
O (^{1}D) SOURCE		REF
▲	NO_2, 2288A	30
△	O_3, 2537A, No He	THIS WORK
□	O_3, 2288A, No He	THIS WORK
●	O_3, 2288A, He	THIS WORK
○	N_2O, 2139A	23

FIGURE 14

k_{9a}/k_9 AS A FUNCTION OF TRANSLATIONAL ENERGY

ratios, Figure 6, the ratio k_{9a}/k_9 as a function of the excess translational energy can be plotted.

The experimental values for various investigations for k_{9a}/k_9 appear to fit the computed curve for the case of one quarter to one third of all collisions between $O(^1D)$ and nitrous oxide resulting in reaction. This fit appears reasonable since the absolute rate constant for the reaction of $O(^1D)$ with N_2O is about 1/4 the collision rate.[28] That the values of k_{9a}/k_9 obtained in different experiments by different investigators fall on this curve, gives credance to the dependency of excess translational energy on the reaction of $O(^1D)$ with nitrous oxide.

The computed curve in Figure 14 is significant in that it predicts a temperature effect on the ratio k_{9a}/k_9. The normal translational energy of a particle is given by the equation $E_T = (3/2)$ RT, where R is the gas constant and T the absolute temperature. At room temperature the normal translational energy has the value 0.9 kcal/mole. Since the value of k_{9a}/k_9 is predicted from Figure 14 to decrease as the energy is increased, an increase in the temperature of the reaction mixture should cause a decrease in the value k_{9a}/k_9. Likewise, the value of k_{9a}/k_9 should increase towards one as the temperature is decreased. Hence, a temperature study of this work would be worthwhile in furthering the understanding of these reactions.

It has been demonstrated that for a translationally excited "hot" $O(^1D)$ atom, the favored mode of reaction with nitrous oxide is to produce nitric oxide. When the $O(^1D)$ atom has the excess translational energy removed, the preferred process is the formation of

nitrogen and oxygen. The competition between ozone and nitrous

oxide for the $O(^1D)$ atom also is dependent on the nature of the

translational energy of the atom. The relative rates of the reactions

involving $O(^1D)$ at the different wavelengths used are listed in

Table 13.

The relative rate of reaction of ozone with $O(^1D)$ is not

as greatly affected by the excess translational energy of the $O(^1D)$

atom as is the rate of reaction of $O(^1D)$ with nitrous oxide. A

reasonable guess for the behavior of the relative rate constants can

be obtained from the data in Table 13 and a knowledge of the system

being studied.

TABLE 13

RELATIVE RATES OF REACTION, $(k_2 + k_{9a} + k_{9b} = 1)$

λ, A	k_2/k_9	k_{9a}/k_{9b}	k_2	k_9	k_{9a}	k_{9b}
2288	6.85	0.53	0.873	0.127	0.044	0.083
2537	2.63	0.59	0.722	0.278	0.103	0.175
2288, (He)	2.13	2.55	0.680	0.320	0.229	0.091
2537, (He)	2.27	4.	0.710	0.290	0.232	0.058

As the amount of translational energy in the $O(^1D)$ atom

increases, so does its velocity. This causes the duration of a collision

to decrease, and hence the time available for the reactions of the

$O(^1D)$ atom decreases. This effect could lead to a decrease in rate

for reactions 2 and 9a as the translational energy is increased. In

reaction 9b the effect could be to initially increase the rate of reaction

due to the increased amount of energy available to overcome the activation energy of the reaction. This initially more than compensates for the shorter time available for the reaction to take place. However, when the energy available to the $O(^1D)$ atom is further increased, the effect of the shorter collision duration causes the value of k_{9b} to drop. A schematic interpretation of the effect of the excess translational energy on the rate constants is shown in Figure 15.
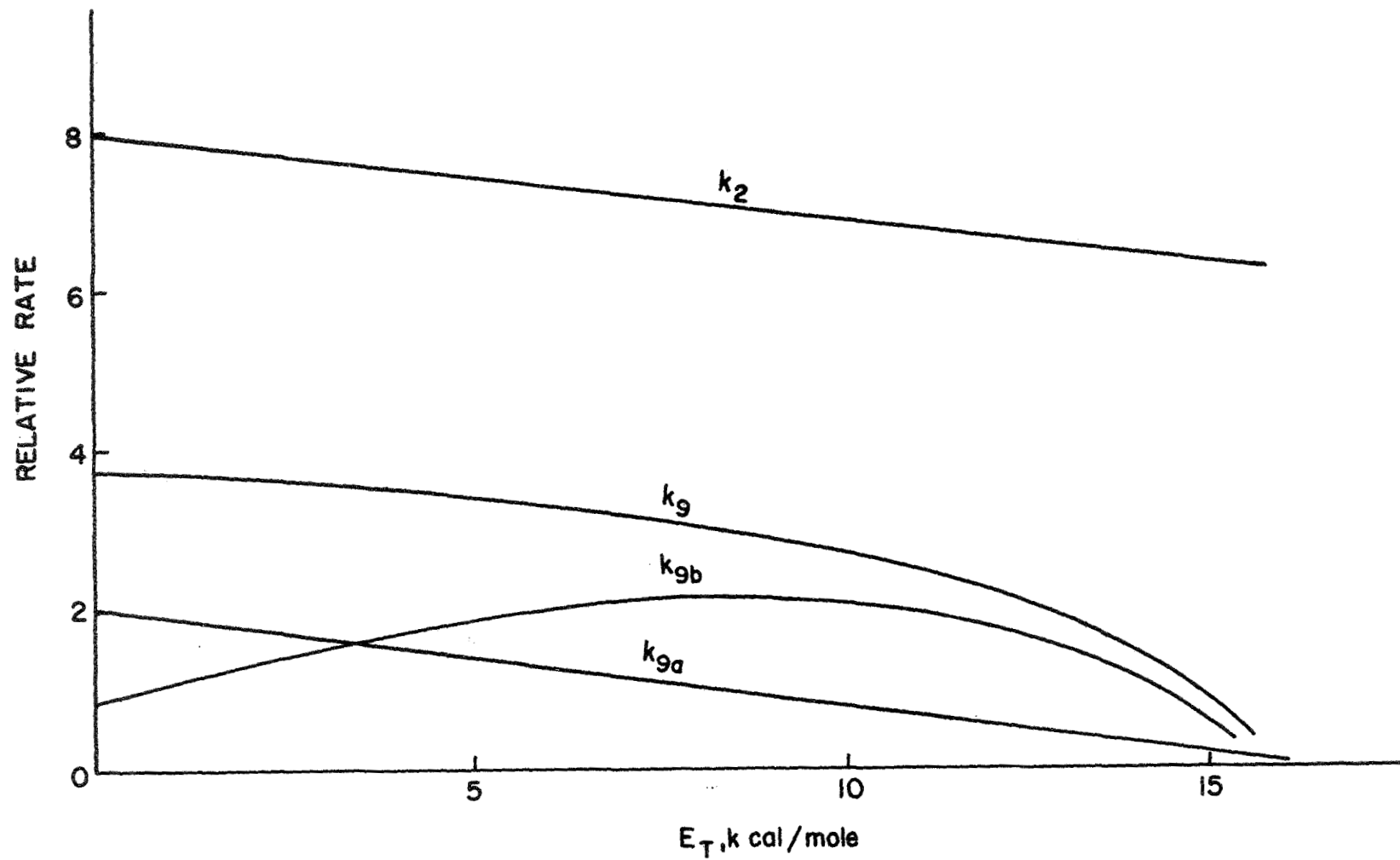
FIGURE 15

RELATIVE RATES OF REACTIONS
(SCHEMATIC INTERPRETATION OF RESULTS)

CHAPTER V

SUMMARY AND CONCLUSIONS

Depending on the method of production, the $O(^1D)$ can possess amounts of translational energy in excess of that obtained from thermal equilibrium. This excess translational energy has been shown in this work to affect the values of the ratios of the various rate constants. This effect, in large part, explains the apparent discrepancy in many of the previous investigations of the ratio k_{9a}/k_{9b}.

By means of competative reaction, it has been found that the rate of reaction of ozone with $O(^1D)$ is faster than that of nitrous oxide with $O(^1D)$. The effect of increasing the excess translational energy of the $O(^1D)$ was to increase the relative rate of the reaction with ozone compared to that with nitrous oxide. This effect was not large until a significant amount of translational energy was present in the $O(^1D)$.

For the reaction of nitrous oxide with the $O(^1D)$ atom, it was found that the ratio of products was dependent on the amount of trans- lational energy of the $O(^1D)$ atom. In the case of the "hot" $O(^1D)$ atom, in the absence of helium, the favored reaction was to give nitric oxide as a product. When a third body was added to remove the excess translational energy of the "hot" atom, the favored mode of reaction was to give nitrogen and oxygen as products.

The results of this work, while only dealing with the reaction of $O(^1D)$ atoms with nitrous oxide and ozone, indicate the need of reevaluating the results of the reaction of $O(^1D)$ atoms with other

reactants. For it appears, that the degree of translational energy possessed by an excited atom should not be overlooked. It should be considered that in the formation of $O(^1D)$ from various sources, the $O(^1D)$ atom can possess translational energies that by thermal means would take thousands of degrees rise in temperature to equal. Therefore, it should not be unexpected that a translational energy effect does exist.

BIBLIOGRAPHY

1. W. D. DeMore and O. F. Raper, J. Chem. Phys., 44, 1780 (1966).

2. M. Nicolet, Ionosphere Research Laboratory Scientific Report 350, Ionosphere Research Laboratory, The Pennsylvania State University (1970).

3. M. Nicolet, Discuss. Faraday Soc., 37, 7 (1964).

4. H. Yamazaki and R. J. Cvetanović, J. Chem. Phys., 40, 582 (1964).

5. J. R. McNesby and H. Okabe, Adv. Photochem., 3, 157 (1964).

6. S. Sato and R. J. Cvetanović, Can. J. Chem., 36, 1668 (1958).

7. B. Mahan, J. Chem. Phys., 33, 959 (1960).

8. W. McGrath and J. McGarvey, Planet. Space Sci., 15, 427 (1967).

9. E. Costellano and H. J. Schumacher, J. Chem. Phys., 36, 2238 (1962).

10. E. Castellano and H. J. Schumacher, Z. Physik. Chem., 65, 62 (1969).

11. J. S. Calvert and J. N. Pitts, Photochemistry, John Wiley and Sons, Inc., New York, (1966), pp. 826.

12. Circular of the National Bureau of Standards, Number 467, 1949.

13. W. B. DeMore and O. F. Raper, J. Chem. Phys., 37, 2048 (1967).

14. R. G. Norrish and R. P. Wayne, Proc. Roy. Soc., Ser. A288, 200 (1965).

15. W. A. Noyes, J. Chem. Phys., 5, 807 (1937).

16. F. Henriques, A. Duncan and W. A. Noyes, J. Chem. Phys., 6, 518 (1938).

17. J. W. Zabor and W. A. Noyes, J. Am. Chem. Soc., 62, 1975 (1940).

18. H. Yamazaki and R. J. Cvetanović, J. Chem. Phys., 39, 1902 (1963).

19. H. Yamazaki and R. J. Cvetanović, J. Chem. Phys., 40, 382 (1964).

20. H. Yamazaki and R. J. Cvetanović, J. Chem. Phys., 41, 3703 (1964).

21. R. J. Cvetanović, J. Chem. Phys., 43, 1850 (1965).

22. K. F. Preston and R. J. Cvetanović, J. Chem. Phys., 45, 2888 (1966).

23. R. J. Greenberg and J. P. Heicklen, Int. Journ. Chem. Kinetics, 2, 185 (1970).

24. J. Heicklen, J. Phys. Chem., 70, 112 (1966).

25. W. B. DeMore and O. F. Raper, J. Chem. Phys., 40, 1053 (1964).

26. D. Biedenkapp and E. J. Bair, J. Chem. Phys., 52, 6119 (1970).

27. D. R. Snelling and E. J. Bair, J. Chem. Phys., 47, 228 (1967).

28. R. A. Young, D. Black, and T. S. Slanger, J. Chem. Phys., 49, 4758 (1968).

29. R. Y. MacDonald, J. Chem. Soc., 1, (1928).

30. K. F. Preston, Private communication, August 21, 1970.

31. M. Zelikoff and L. M. Aschenbrand, J. Chem. Phys., 5, 807 (1937).

32. S. W. Benson, The Foundation of Chemical Kinetics, Chapter 8, McGraw-Hill Book Co., Inc., New York, (1960).

33. R. A. Svehla, "Thermodynamic and Transport Properties for the Hydrogen-Oxygen System," NASA SP-3011, 1964.

34. E. H. Kennard, The Kinetic Theory of Gases, McGraw-Hill Book Co., Inc., New York, (1938).